1-1-1983

Deflection of prestressed concrete beaks.

Douglas C. Stumpp

DEFLECTION OF PRESTRESSED CONCRETE BEAMS

by

Douglas C. Stumpp

A Thesis

Presented to the Graduate Committee

of Lehigh University

in Candidacy for the Degree of

Master of Science

in

Civil Engineeering

Lehigh University
1983

CERTIFICATE OF APPROVAL

This thesis is accepted and approved in partial fulfillment of the requirements for the degree of Master of Science in Civil Engineering.

Sept. 16, 1983
(date)

Professor in Charge

Chairman of Department

ACKNOWLEDGEMENTS

The author would like to thank Dr. Ti Huang for his supervision of the work and review of the manuscript.

Research for this thesis was conducted at the Fritz Engineering Laboratory at Lehigh University. Dr. Lynn S. Beedle is the director of Fritz Laboratory. Dr. David A. VanHorn is chairman of the department of Civil Engineering at Lehigh University.

The author would also like to thank his office-mates, in particular, Mr. Peter Keating for his help with the figures and Mr. John Brun for his comments. Special acknowledgement goes to Mr. D. McDuff.

Table of Contents

List of Tables

List of Figures

ABSTRACT

Previous research has lead to a procedure for the estimation of losses in prestressed concrete beams. This procedure is applicable to all types of construction-- pretensioned, post-tensioned, pre-post-tensioned and segmental. It is based on empirically developed stress-strain-time relationships for steel and concrete that are combined with equilibrium and compatibility conditions to obtain the stresses and strains at a cross-section at a given time. Here, this procedure is employed to enable a direct determination of midspan deflection at any time during the useful life of a prestressed concrete member.

The variation of prestress force along the span is found to be small, thus allowing a parabolic approximation to the curvature diagram for straight and parabolic tendons. The midspan deflection of the beam is then computed using moment-area principles. For harped tendons, a correction factor is introduced to account for the nonparabolic prestress curvature diagram. Two typical examples are included to illustrate the application of the procedure, and to compare results.

1. INTRODUCTION

1.1 Background

In any structural design there are two criteria that must be satisfied to assure a good design-- strength and serviceability. First, a structure must have adequate strength to carry the design loads. This does not, however, guarantee a good design. The overall in-service performance of a structure must be considered. For instance, in a typical flat roof building it is important to consider the deflections of the roof beams. Even when the beams are designed to have adequate strength to carry all loads, if they deflect too much, drainage problems could arise. By limiting the deflection, then, a serviceability requirement will be satisfied.

For prestressed concrete beams, the downward deflection caused by loads is not the only critical behavior. The upward deflection, or camber, due to prestress must also be controlled. For example, in bridge beams large downward deflections may cause drainage problems or unwanted cracking. Excessive camber, on the other hand, could result in an uneven road surface. Because of the shrinkage and creep of concrete, as well as the gradual loss of prestress with time, the beam deflection, or camber, changes continuously. Consequently, an accurate estimation of the deflection is necessary throughout the life of the member.

The deflection of a beam is controlled by the distribution of

curvature along its length. For a prestressed concrete beam the curvature distribution can be determined only if the prestress force is known at every cross-section along the span. Unfortunately, the prestress force will change with time. Thus the accuracy of deflection calculations depends upon the ability to accurately estimate the prestress losses and the concrete strains at any time.

1.2 Objectives

The principal objective of this report is to determine the midspan deflection of a prestressed beam using a previously developed procedure for estimating prestress losses. To attain this end, the following steps are necessary:

1. Evaluate the magnitude of the variation of the prestress force along the span.
2. Develop the curvature diagram of the prestressed beam.
3. Apply moment-area principles to calculate the deflection.
4. Modify the existing computer program to carry out objectives 2 and 3 for any time during the life of the beam.

1.3 Definitions and Sign Convention

In the development of the loss estimation procedure to be used, the definitions of several terms were clearly defined to avoid confusion. These definitions will be used within this report and are as follows:

Prestress: Prestress is defined as the stress in steel and concrete at any time, excluding the stresses caused by the applied loads. Thus, the prestress is computed by subtracting the stress due to the applied loads, including the member's selfweight, from the total stress.

$$f_{prestress} = f_{total} - f_{loads}$$

Losses: Loss of prestress is defined as the reduction in steel prestress occurring after the initial jacking. The major components of prestress losses are relaxation of steel, creep and shrinkage of concrete, elastic shortening and frictional and anchorage losses in post-tensioning.

Sign Convention: The positive direction for applied loads at a cross-section is shown in Figure 1. Figure 1 also shows the sign convention for deflections; that is, positive deflection is taken downward in the positve y-direction. Upward deflection or camber is negative.

2. REVIEW OF PREVIOUS WORK

2.1 Current Methods to Compute Deflections

Several methods of varying complexity are currently available for deflection calculations of prestressed beams. The degree of complexity depends on the accuracy with which prestress losses and creep strains are determined over time.

The simplest method considers only two stages-- the initial and ultimate stages [1]. The initial stage occurs at transfer when the prestress force is P_i. The ultimate stage occurs after all losses when the prestress force is P_e. Prestress losses are all lumped together as a percentage of the initial stress P_i. A creep coefficient is used to reflect the creep effects. The resulting ultimate deflection due to sustained effects is then

$$\Delta = -\Delta_{pe} - \frac{\Delta_{pi} + \Delta_{pe}}{2} C_u + \Delta_D(1 + C_u) \qquad (2\text{-}1)$$

where

Δ = the total deflection at ultimate.

Δ_{pe} = the deflection due to P_e.

Δ_{pi} = the deflection due to P_i.

Δ_D = deflection due to all sustained loads, including selfweight.

C_u = ultimate creep coefficient.

The negative signs in the first and second terms indicate upward camber. Note also that in the second term the creep effect on Δ_p is approximated by applying the coefficient C_u, determined for constant stress conditions, to the average of the initial and final prestress deflections. Actually creep occurs under a decreasing prestress force.

A more involved method uses an incremental time step approach to compute the curvature of a cross-section [1]. For each time-step, the change in curvature due to prestress loss and creep strain is determined. This change in curvature is added to the curvature at the beginning of the time-step to obtain the curvature at the end of the time-step. By repeating this process for various cross-sections along the span, the curvature diagram for a given time can be constructed. The deflection is computed by integrating this curvature diagram. Repeating this procedure for additional intervals then produces information on deflection throughout the member's life. Obviously, the ammount of calculations required makes this method impractical for manual computations-- a computer is required. Furthermore, this method requires that the time dependent behavior of the concrete and steel materials be known in detail. That is, the creep and shrinkage behavior of the particular concrete must be known along with the relaxation characteristics of the prestressing steel.

2.2 General Procedure to Estimate Prestress Losses

The two methods described above differ only by the way prestress losses are accounted for. In the first method, the total prestress loss is estimated as a sum of the component losses-- creep, shrinkage, etc. The interrelation between the components is not considered directly. The second method uses a cumulative approach to determine the curvatures, and the accuracy of the results depends directly on the number and magnitude of time steps. A recently proposed procedure offers an alternative, however, that automatically takes the interaction among loss components into account and also does not require a summation process to obtain the prestress at any time [2].

In a 14 year research effort carried out at Lehigh University, the new general procedure to estimate prestress losses was developed. This method is based upon empirical stress-strain-time relationships for steel and concrete materials. It provides a rational method to determine the stress and strain distribution in concrete at any time. As developed, the general procedure is applicable to all types of prestressed members-- pretensioned, post-tensioned, pre-post-tensioned, and segmental. Appendix B gives the empirical stress-strain-time equations and a brief outline of the general procedure. A detailed description of the general procedure and its development is given in references 2,3,5,6. Using this method, the deflection of a beam may be determined once the stresses and strains are known at each time.

2.3 Assumptions

A computer program has been developed for the general procedure of prestress loss estimation, mentioned in the previous section [3]. Several assumptions were employed in the development of the program. They are explicitly stated here to indicate the limitations of the program, and clearly, they also apply for the determination of deflections to be discussed in Chapter 4.

Linear Strain Distribution

A linear strain distribution is assumed across the beam depth. This was implied in the previous assumption of a linear stress distribution in Appendix B. For a linear strain distribution, the curvature is computed by equation (2-2).

$$\Phi = \frac{S_{c1} - S_{c2}}{h} \qquad (2\text{-}2)$$

where

Φ = curvature of the cross-section, in^{-1}.

S_{c1} = concrete strain at the top of the beam, contraction positive.

S_{c2} = concrete strain at the bottom of the beam, contraction positive.

h = depth of the beam, inches.

A negative curvature, therefore, corresponds to a negative deflection (camber).

It is important to note that the linear concrete stress-strain relationship is valid for a fixed time only. With the passing of time, the concrete stress will gradually decrease as losses occur. The concrete strain, on the other hand, will increase with time as creep occurs. Obviously, the linearity will not hold among values at different times.

Simple Beams

A simply supported prismatic beam is assumed in the development of the program. Segmental construction is accounted for by inputting a new span length for each additional segment, computing the additional selfweight moment, and analyzing the new span by the general procedure.

Uncracked Behavior

The member is assumed to remain uncracked under the action of prestress and sustained loads. Live load effects are not included because they do not affect the long-term behavior of the beam. When needed, the instantaneous deflection due to live load can be calculated using any conventional method. A reduced effective moment of inertia, as suggested by Branson, may be used in case flexural cracks develop under live load [4]. Also, concrete is assumed to be bonded to steel either directly (pretensioning) or by grouting (post-tensioning).

Parabolic Tendon Profile

The profile of post-tensioned tendons is assumed to be parabolic over the entire span. This assumption was used previously in the subroutine ANCFR for the determination of losses due to anchorage seating and friction and will be maintained for the deflection calculations. For pretensioned members, information on the tendon profile is not needed for loss estimation but is needed for deflection calculations. Further discussion is given in section 4.3.

3. VARIATION IN PRESTRESS FORCE ALONG THE SPAN

One of the primary concerns in this study was the effect of the variation in prestress force along the span. The variation in prestress force from support to midspan has a direct affect on the curvature diagram and hence the deflection of the beam. This can best be illustrated by an example.

Consider a prestressed beam with straight tendons as shown in Figure 2. Initially the prestress force is constant over the entire span and the corresponding curvature due to prestress, Φ_P, is also constant, Figure 2a. Upon the application of selfweight and sustained loads, a parabolic curvature diagram, Φ_D, is superimposed upon the prestress curvature. The resulting total curvature diagram, Φ_T, is also parabolic as shown in Figure 2c. As time progresses, long term prestress losses would cause the prestress force to vary along the span; the resulting prestress curvature, Φ_p, would not be constant. Figure 2d shows the curvature diagram for prestress after losses. The curvature diagram due to sustained loads remains parabolic, Figure 2e. The total curvature diagram (2f) is not exactly parabolic and integration is not feasible. To facilitate computation of the midspan deflection, however, a parabolic approximation to the total curvature diagram is proposed. One of the first tasks of this study, then, was to determine the error introduced by this assumption. An estimate of the error can be obtained by determining the magnitude of the variation in prestress force along the span.

A sample beam cross-section and span were chosen to estimate the variation in prestress force. Figure 3 shows the beam section used and its properties. The existing computer program FOUR02 (reference 5) was used to evaluate the prestress force at the support and at midspan for the ten cases shown in Table 1. The variation in prestress force from support to midspan was calculated over the 100 year life of the beam. The worst case was case 2 -- a pretensioned beam with straight tendons. As shown in Table 2, the maximum prestress variation for this case was 7.11 % after 100 years.

The sample beam, as shown in Figure 3, used concrete exhibiting lower bound prestress losses. Another concrete that exhibits greater losses may cause greater variation in prestress along the span. For this reason, case 2 was repeated using upper bound concrete. The variation in prestress after 100 years was found to be 10.6 % . The relatively small variation in prestress indicates that a parabolic approximation to the total curvature diagram is acceptable.

The data for the ten cases shows that the tendon profile influences the variation in prestress along the span. Straight tendons seem to produce the greatest variation. By examining the two profiles, we can see that these results are reasonable.

3.1 Straight Tendons

At first, it was thought that after losses, the prestress force at midspan, P_{mid}, would be less than the support prestress, P_{sup}. The reasoning was that the increased steel force at midspan caused by the sustained loads would promote greater loss of prestress from relaxation. The more dominant influence of creep, however, caused P_{mid} to be greater than P_{sup}.

Figure 4 shows a plot of prestress versus time for the support and midspan sections for the sample beam cases 1 and 2. At transfer (time zero), P_{sup} is equal to P_{mid} for pretensioned beams (assuming the development length of the steel is small at the support). For post-tensioned beams, P_{sup} may differ from P_{mid} as the result of frictional and anchorage seating losses that occur during tensioning. As Figure 4 shows, the rate of prestress loss is greater at the support. This can be explained by realizing that the application of sustained loads actually reduces creep losses at midspan. This is illustrated in Figure 5. Prior to the application of sustained loads, the strains at the support and midspan are identical as shown by the solid lines in Figure 5a. With the application of sustained loads, the concrete elastic strain at midspan, S_{ci}, is reduced by the strain S_D caused by the loads. Assuming creep strain is directly related to the elastic strain, the creep loss at midspan is less than that at the support, $(S_{crm} < S_{crs})$.

3.2 Parabolic Tendons

A parabolic tendon profile has several advantages over straight tendons. From a strength point of view, a parabolic profile more accurately counterbalances the applied loads and avoids large tensile stresses in the top fibers at the support. The more uniform stress distribution at the support also reduces the creep strains. As a result, the rate of prestress loss at the support may or may not be as fast as at midspan. Figure 6 shows a plot of prestress versus time for the midspan and support sections for case 5 (no slab) and case 6 (slab at 40 days). For both of these cases the reduced prestress eccentricity at the support results in a greater prestress force at the support. For case 5 the midspan and support prestress decrease at about the same rate. When the additional slab load is added in case 6, the prestress loss is reduced and the rate of loss at the support becomes greater than at midspan. As figure 6 shows, the variation in prestress is still relatively small-- under 5 % in each case-- and a parabolic approximation appears satisfactory.

3.3 Additional Discussion

As a further check of the parabolic approximation, the computer program was used to compute the total curvature at the quarter point of the span. This value was compared to the curvature obtained by the parabolic approximation. For straight and parabolic tendons, the two values compared favorably. Straight tendons showed less

than 2 percent difference after 100 years. Parabolic tendons showed less than 4 percent difference. However, the curvatures for harped tendons showed poor correlation to the parabolic approximation. To allow the use of harped tendons, then, a correction factor was derived. Section 4.3 describes its derivation and use.

4. EXTENSION OF THE COMPUTER PROGRAM

4.1 Curvature Approximation

Having chosen a parabolic approximation to the total curvature diagram, the curvatures of three cross-sections along the span are needed to define the curve. The curvatures of the two supports and midspan were selected. Assuming a symmetric tendon profile and applied loading of the beam, the curvatures of the two supports are the same. Consequently, it is necessary to calculate the curvature at only two locations-- at a support and at midspan. The equation of the parabolic approximation is derived in Appendix C.

4.2 Calculation of Midspan Deflection

The midspan deflection of a symmetric simple beam can easily be computed for a parabolic curvature diagram. Figure 7 shows that for a symmetric deflected shape the midspan deflection, Δ, is equal to the tangential deviation of the support, point A, with respect to the midspan section, point C. To find the tangential deviation, $t_{A/C}$, we can use moment-area principles. That is

$$\Delta = t_{A/C} = \text{first moment of the area of the curvature diagram, } \Phi_T, \text{ between A and C, about point A.}$$

Evaluating the first moment, as shown in Appendix C, we arrive at a

solution

$$\Delta = \frac{L^2}{48} (\Phi_1 + 5\Phi_2) \qquad (4\text{-}1)$$

where

Δ = midspan deflection, inches.

L = span length, inches.

Φ_1 = curvature of the support section, in^{-1}.

Φ_2 = curvature of the midspan section, in^{-1}.

Note that the symmetric Φ_T diagram allows the computation of Δ using only two points on the curvature diagram.

4.3 Correction for Harped Tendons

A harped tendon profile causes a distinctly non-parabolic prestress curvature diagram. Figure 8 shows a general curvature diagram for harped profile. To calculate the deflection then, a correction is needed for equation (4-1) for total deflection.

Consider the general case of pre-post-tensioned construction. The total deflection at any time may be written as

$$\Delta_T = \Delta_D + \Delta_{PrH} + \Delta_{PsP} \qquad (4\text{-}2)$$

where

Δ_T = total deflection.

Δ_D = deflection caused by all sustained loads including selfweight.

Δ_{PrH} = deflection due to harped tendons.

Δ_{PsP} = deflection due to straight or parabolic tendons.

In this formulation, each pretensioning stage may have any tendon profile-- straight, harped, or parabolic. All post-tensioning stages must have either straight or parabolic tendons (corresponding to a parabolic curvature diagram).

Next, define a factor as

$$R_t = \frac{\Delta_{PrH}}{\Delta_{PrP}} \tag{4-3}$$

where

Δ_{PrP} = the deflection due to pretensioning stages for a parabolic profile with the same pretensioning force and eccentricity at the support and midspan as Δ_{PrH}.

The terms Δ_{PrH} and Δ_{PrP} are determined by moment area principles (see Appendix C) and substituted into equation (4-3) to obtain:

$$R_t = \frac{8\Phi_{Pr1}(z/L)^2 + \Phi_{Pr2}[6 - 8(z/L)^2]}{\Phi_{Pr1} + 5\Phi_{Pr2}} \tag{4-4}$$

where

Φ_{Pr} = curvature due to pretensioning stages. The

subscripts 1 and 2 denote support and midspan sections, respectively.

z = distance from the support to the harping point.

L = span length.

To determine Δ_T, equation (4-2) is rewritten as

$$\Delta_T = \Delta_D + R_t \Delta_{PrP} + \Delta_{PsP} \tag{4-5}$$

Using equation (4-1) we can determine the component deflections to be

$$\Delta_D = \frac{5L^2}{48} \Phi_{D2} \tag{4-6}$$

$$\Delta_{PrP} = \frac{L^2}{48} [\Phi_{Pr1} + 5 \Phi_{Pr2}] \tag{4-7}$$

$$\Delta_{PsP} = \frac{L^2}{48} [\Phi_{Ps1} + 5 \Phi_{Ps2}] \tag{4-8}$$

where

Φ_{D2} = midspan curvature due to all sustained loads.

Φ_{Ps} = curvature due to post-tensioning stages.

Subscripts 1 and 2 denote the support and midspan sections, respectively.

The computer program, as developed, can readily compute the total curvatures at any time. These can be written as the sum of the component curvatures.

That is

$$\Phi_1 = \Phi_{Pr1} + \Phi_{Ps1} \tag{4-9}$$

$$\Phi_2 = \Phi_{D2} + \Phi_{Pr2} + \Phi_{Ps2} \tag{4-10}$$

where

Φ_1 = the total curvature at the support.

Φ_2 = the total curvature at midspan.

Substituting equations (4-6), (4-7), and (4-8) into (4-5) and using the relationships in equations (4-9) and (4-10), we can arrive at the following expression for Δ_T:

$$\Delta_T = \frac{L^2}{48} [\Phi_1 + 5\Phi_2 + \Sigma\{(R_t - 1)(\Phi_{Pr1} + 5\Phi_{Pr2})\}] \tag{4-11}$$

Note that the summation in equation (4-11) allows the use of several pretensioning stages with different tendon profiles.

To find Δ_T the pretensioning curvatures must be computed in addition to the total curvatures. This is accomplished by performing a analysis of the concrete section subjected to an externally applied axial load equal to the pretensioning force after losses.

The stresses obtained by this analysis are used in equation (B-2) to obtain the concrete strains. Appendix C shows that the

pretensioned curvature at any section can be found by

$$\Phi_{Pr} = \frac{- Q_2 P_r e_r}{100 I_c} \qquad (4\text{-}12)$$

where

P_r = total force contributed by all pretensioning stages, after losses.

e_r = eccentricity of pretensioning force, positive in the positive y-direction.

I_c = net concrete moment of inertia.

Q_2 = factor defined in Appendix C that accounts for creep in concrete.

Appendix C gives a detailed derivation of equation (4-12).

4.4 Modifications to the Computer Program

The computer program, as previously developed, deals with only the midspan section. For any time, the section is analyzed using the procedure described in Appendix B and a linear stress distribution is obtained. In order to calculate the total curvature of a cross-section, the program was modified to calculate the concrete strains at the top and bottom of the beam using the stress-strain-time relationship for concrete. The curvature of the cross-section is then calculated using equation (2-2).

To construct an approximate curvature diagram, the program had

to provide the total curvature of the support and midspan sections. Thus, it was modified to analyze both cross-sections and compute both curvatures at any time. After the curvatures of both cross-sections are computed, subroutine DROP is called. Subroutine DROP accepts as input the total curvatures, Φ_1, Φ_2, and the current prestress force due to pretensioning stages (P_{r1}, P_{r2}). It then calculates the curvature due to pretensioning stages, Φ_{Pr}, at each cross-section, using equation (4-12). The factor R_t is then computed and applied to the curvature of each pretensioning stage. Finally, the midspan deflection is found using equation (4-11).

5. EXAMPLES AND COMPARISON OF RESULTS

5.1 Deflections of an Existing Bridge Girder

In reference 7, Branson reported on measured deflections of several bridge girders with 86 feet spans. The girders were made of sand-lightweight concrete, pretensioned using harped tendons. A seven inch slab of normal weight concrete was cast to act compositely with the girders. For the purpose of comparison, interior girder number 153 was analyzed by the program developed in this study. Figure 9 gives the cross-section of the girder, its properties and loads.

The comparison of results as seen in Figure 11 shows the measured data points lying below the computed curve. This can be attributed to the differences in concrete loss characteristics. For the loss estimation procedure used here, the concrete losses were based upon typical normal weight concrete used in Pennsylvania. In this example, lower bound concrete loss characteristics were used. As the actual concrete in the bridge girders was sand-lightweight concrete with a lower modulus of elasticity than the Pennsylvania concrete, the differences are understandable. The lower modulus is reflected by the larger initial camber and the greater decrease in camber upon casting the slab (Figure 11). It may be expected that better comparisons will be obtained if more suitable concrete characteristic coefficients for lightweight concrete are used in the proposed procedure.

5.2 An Idealized Example

As another example, the method developed herein was applied to the beam shown in Figure 10. This beam has a span of 65 feet and is pretensioned using straight tendons. Reference 8 presents the results of an analysis of this beam using a computer program PBEAM. The results of this analysis are shown in Figure 12 together with the results from the program FOUR02 developed here.

Again, the larger initial camber from PBEAM indicates that a smaller modulus of elasticity was used in that program. The differences in the curves, however, are not only the result of different concretes used in the analyses. The mathematical time-functions used to compute prestress losses are probably not the same. This is indicated after the additional loading where the PBEAM curve seems to approach a limiting value very early. The FOUR02 curve, on the other hand, shows continued growth of the deflections. To verify the accuracy of either method, then, it would be helpful if more experimental data were available for long-term deflections.

6. SUMMARY AND CONCLUSIONS

To summarize, an investigation of the variation of prestress along the span was performed. For any prestressed beam, this variation in prestress was found to be small throughout the life of the beam. For parabolic and straight tendons, the curvature diagram of the beam could then be approximated by a parabola at any time. For harped tendons, the parabolic approximation could be used provided a correction factor was applied to account for the non-parabolic nature of the prestress curvature diagram. The deflection was then computed from the curvature diagram using moment-area principles.

Finally, the existing program FOUR02 has been modified to compute the deflections. These modifications entail first computing the concrete strains and total curvatures of the midspan and support section. Next, subroutine DROP was added to apply the correction factor for harped tendons and compute the deflections. Further modifications include allowances for harped, straight, or parabolic tendons for each stage of pretensioning. Only straight or parabolic tendons are allowed for any post-tensioning stages.

On the whole, the method presented here should provide a reasonable estimate of deflections in beams using Pennsylvania concrete. To provide a more accurate solution for other concretes, the characteristc coefficients in Table 4 may be determined for the

particular concrete. Also, program FOUR02 could be further enhanced by modifying it to account for the variability of the modulus of concrete with time. This modification could take the form of a time function applied to the initial modulus of elasticity which would be accepted as input.

The second example illustrates the need for more data measurements over a period of many years. From this data, the true deflection-time curve of deflections could be found.

TABLES

Case	Tensioning Mode(s)	Number of Strands	Tendon Profile d_1	d_2	Additional Loads
1	pre-	70	50.80	50.80	--
2	pre-	70	50.80	50.80	slab @ 40 days
3	post-	70	50.80	50.80	--
4	post-	70	50.80	50.80	slab @ 40 days
5	pre-	70	31.04	50.80	--
6	pre-	70	31.04	50.80	slab @ 40 days
7	post-	70	31.04	50.80	--
8	post-	70	31.04	50.80	slab @ 40 days
9	pre- post-	49 24	50.80 50.80	50.80 50.80	slab @ 40 days
10	pre- post-	49 24	50.80 31.04	50.80 50.80	slab @ 40 days

All post tensioning stages occured at 7 days except cases 9 and 10 which occured at 30 days.

Additional load is that load applied in addition to the beam selfweight.

Table 1: Sample Cases

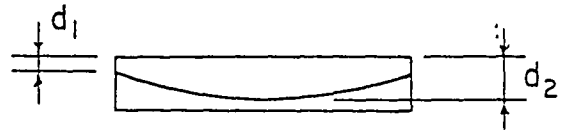

Relative variation in prestress force with time.

$$\%\Delta P = \frac{P_{mid} - P_{sup}}{P_{sup}} (100)$$

Case	Time After Transfer (days) 0	30	500	3000	10000	36500
1	0.0	1.08	2.38	3.24	3.82	4.47
2	0.0	1.08	3.78	5.16	6.09	7.11
2a	0.0	1.60	5.35	7.40	8.88	10.60
2b	0.0	1.30	3.95	5.30	6.26	7.34
3	--	-0.76	0.44	1.16	1.66	2.20
4	--	-0.76	1.64	2.81	3.60	4.46
5	-3.02	-3.70	-4.09	-4.23	-4.27	-4.28
6	-3.02	-3.70	-2.78	-2.44	-2.18	-1.86
7	--	-2.42	-2.92	-3.10	-3.17	-3.21
8	--	-2.42	-1.76	-1.52	-1.32	-1.07
9	0.0	--	2.65	3.96	4.84	5.79
10	0.0	--	0.24	0.95	1.46	2.03

Case 2a used upper bound concrete loss characteristics.

Case 2b used average concrete loss characteristics.

All other cases used lower bound concrete losses.

Table 2: Results of Ten Cases

Instantaneous Stress-Strain Relationship

All Manufacturers	A_1 = -0.4229	
	A_2 = 1.21952	
	A_3 = -0.17827	

Relaxation Coefficients - Stress Relieved Strands

Size	Manufacturers	B_1	B_2	B_3	B_4
7/16 in.	B	-0.05243	0.00113	0.11502	0.05228
	C	-0.04697	-0.01173	0.10015	0.05943
	U	-0.06036	0.00891	0.12068	0.02660
	ALL	-0.05321	0.00291	0.11294	0.03763
1/2 in.	B	-0.06380	0.00359	0.12037	0.05673
	C	-0.07880	-0.00762	0.14598	0.05920
	U	-0.06922	0.00844	0.13645	0.04394
	ALL	-0.07346	0.00620	0.13847	0.04608
ALL	ALL	-0.05867	0.00023	0.11860	0.04858

Low-Relaxation Strands

7/16 in.	L	-0.00412	0.00142	0.02203	0.01605
1/2 in.	L	-0.02672	0.01399	0.04435	0.00923
	ALL	-0.01403	0.00609	0.03245	0.01395

Table 3: Coefficients for Prestressing Steel

Coefficients		Upper Bound	Lower Bound	Combined
Elastic Strain	C_1*	0.02500	0.02105	0.02299
Shrinkage	D_1	-0.00668	-0.00066	-0.00289
	D_2	0.02454	0.01500	0.02031
Creep	E_1	-0.01280	-0.00664	-0.01592
	E_2	0.00675	-0.00331	0.00649
	E_3	-0.00600	-0.00371	0.00256
	E_4	0.01609	0.01409	0.01153

*Note: $C_1 = 100/E_c$ where E_c is modulus of elasticity for concrete, in ksi

Table 4: Characteristic Coefficients for Concrete

FIGURES

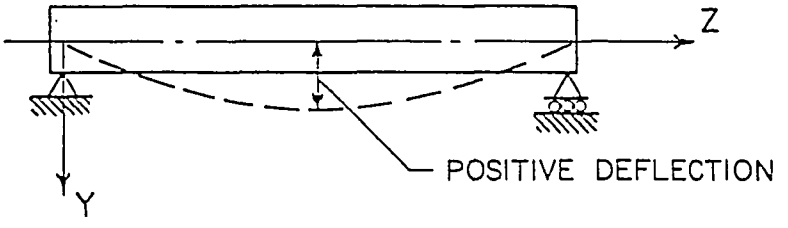

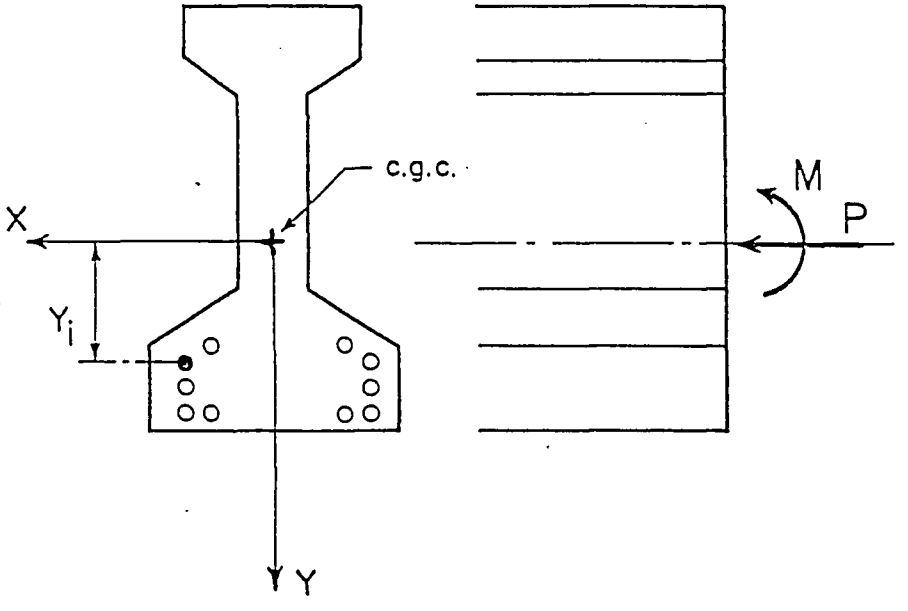

Figure 1: Sign Convention

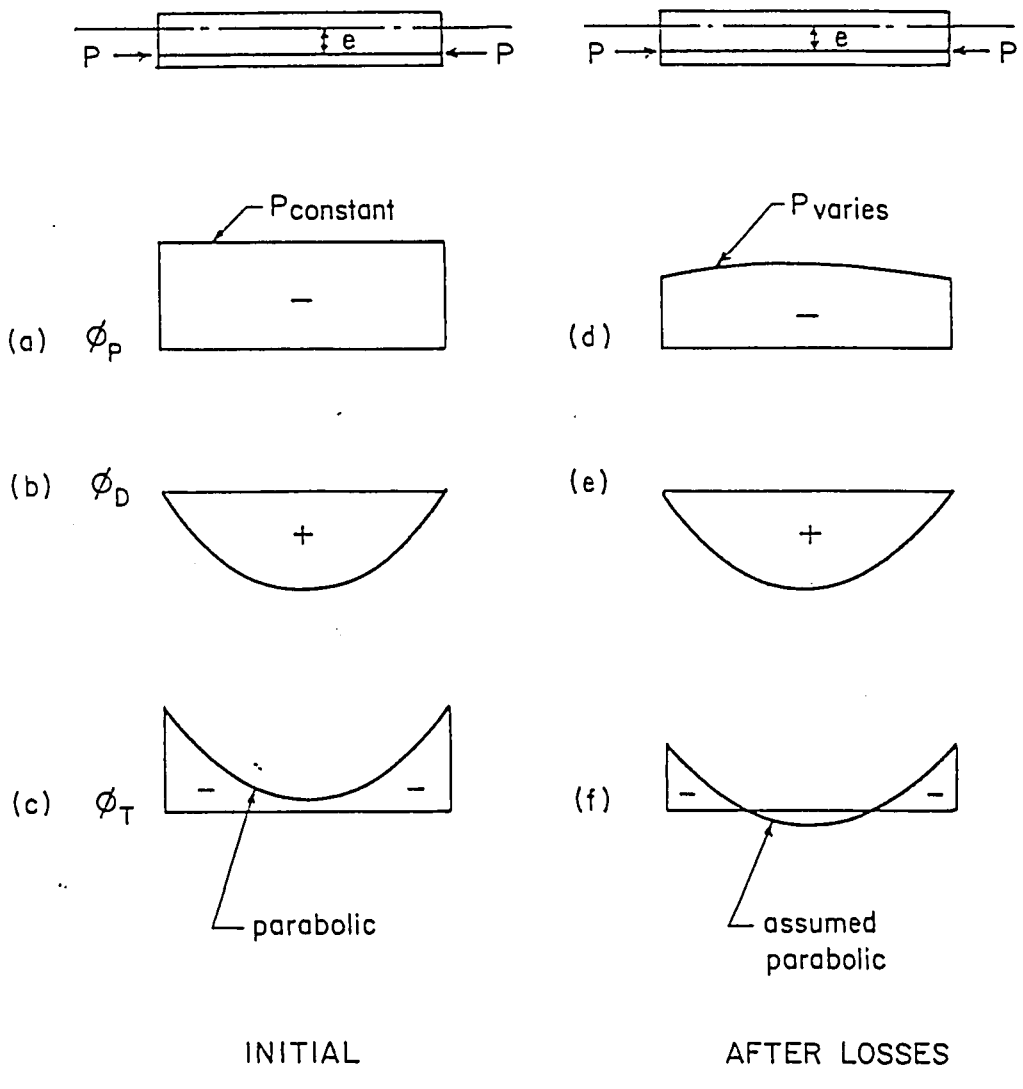

Figure 2: Effect of Prestress Variation on Total Curvature Diagram

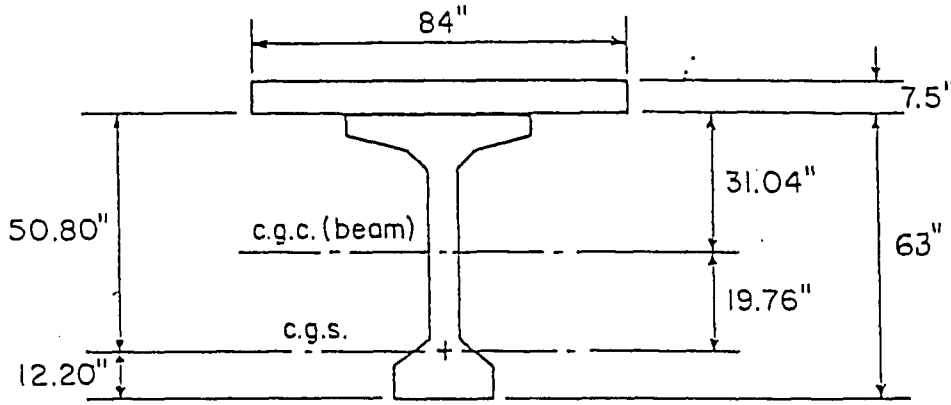

Concrete Characteristics: Lower Bound Losses
$n_i = 5$
$E_{ci} = 4750$ ksi

Steel Characteristics: Average for 270 K stress-relieved strands.

Strand Properties: Area = 0.117 in^2 per strand
$f_{pu} = 265$ ksi

Precast Concrete Section: AASHTO Type V

Area = 1013 in^2
I = 521163 in^4
f'_c = 6250 psi

Tensioning Stress $f_{pi} = 0.70\ f_{pu} = 185.5$ ksi

Member Selfweight Moment = 16790 kip-in

Deck Slab: Slab weight moment = 10440 kip-in
f'_c = 3500 psi
Total thickness = 7.5 inches
Structural thickness = 7.0 inches

Span Length = 103 feet

Figure 3: Sample Beam Properties

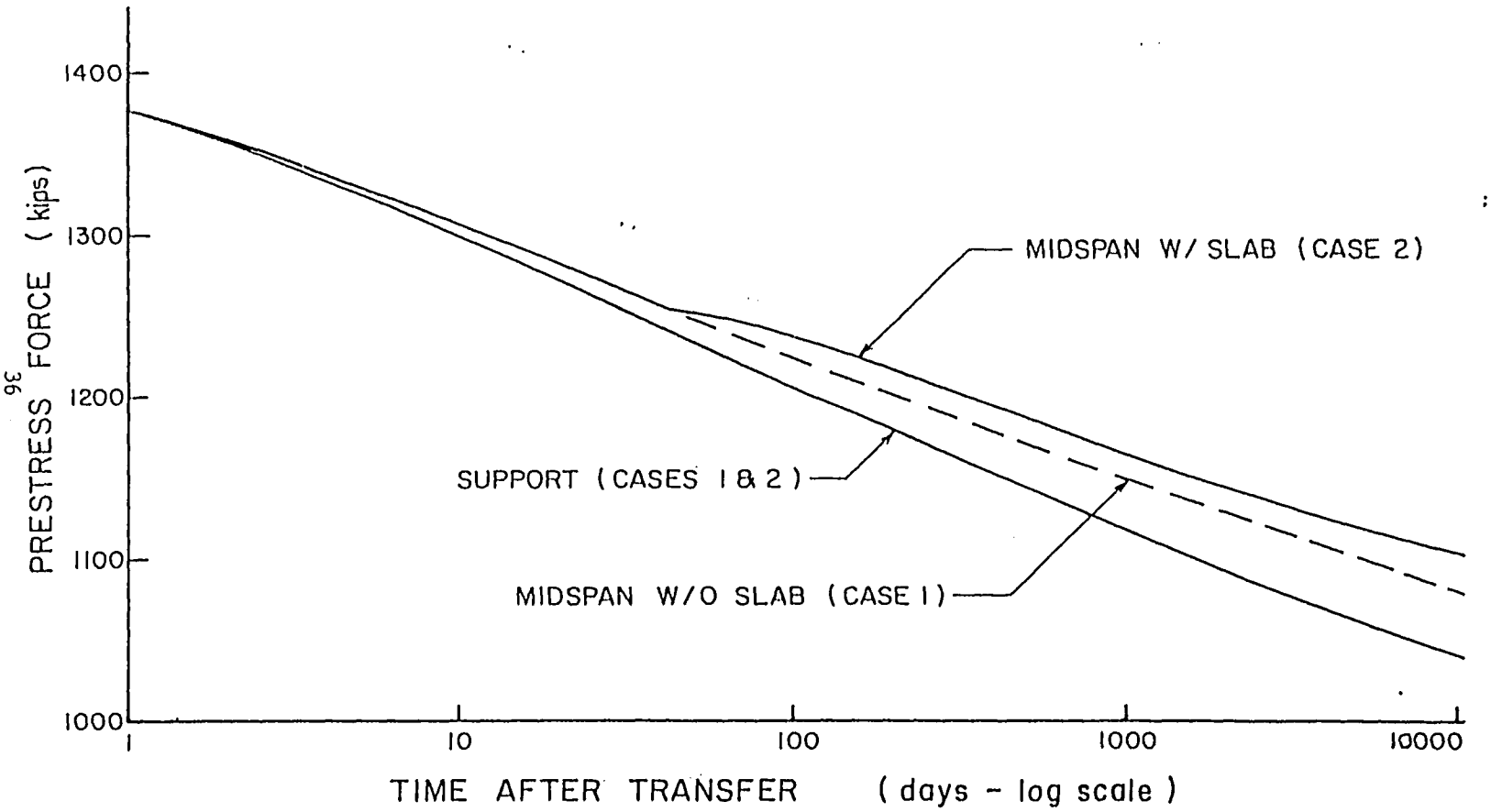

Figure 4: Variation of Prestress with Time- Straight Tendons

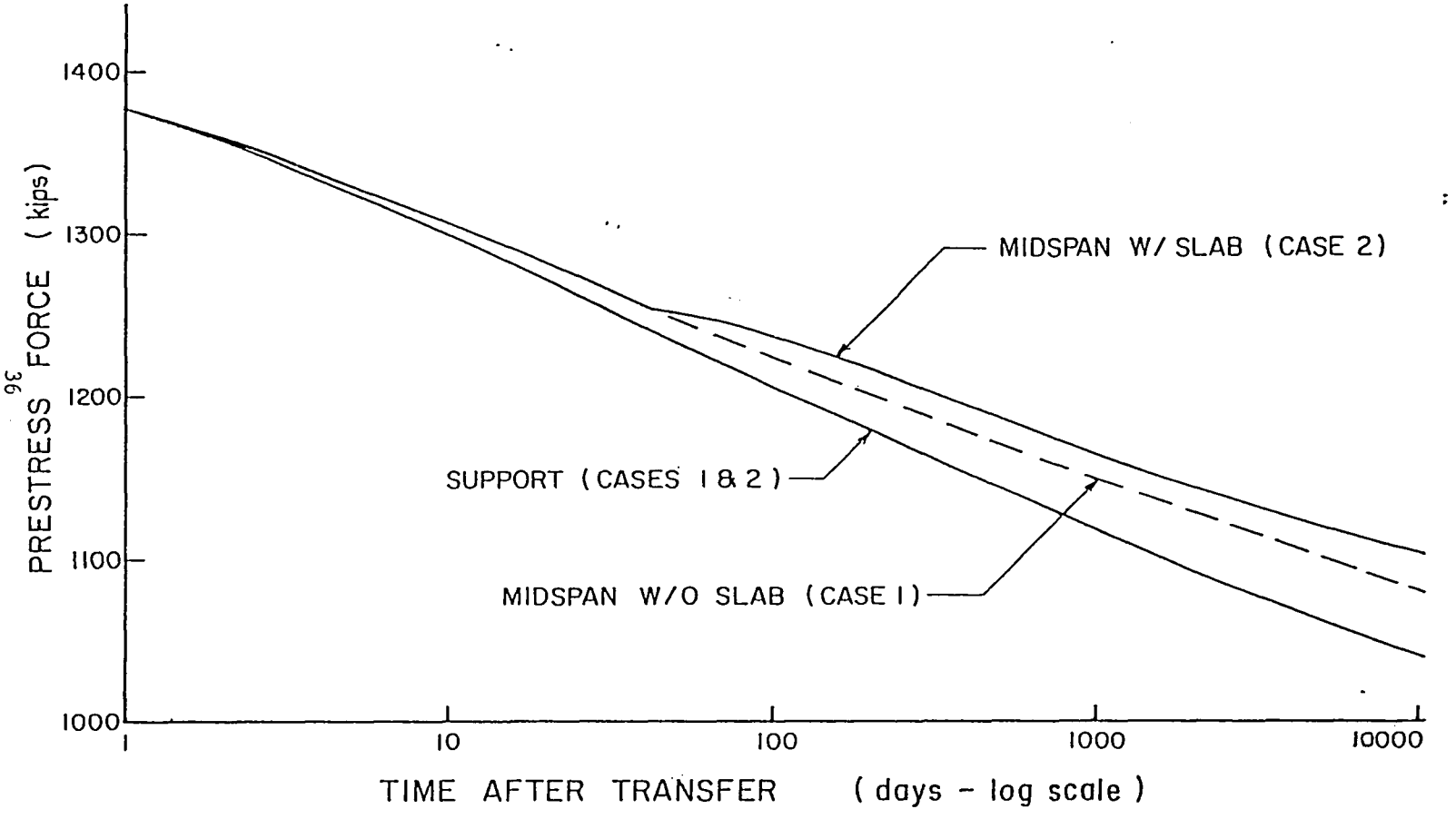

Figure 4: Variation of Prestress with Time- Straight Tendons

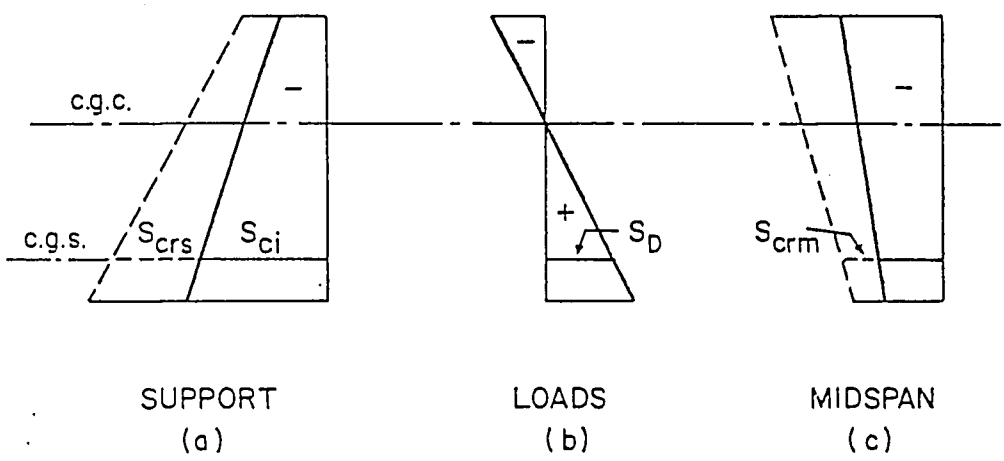

Figure 5: Strains in a Beam With Straight Tendons

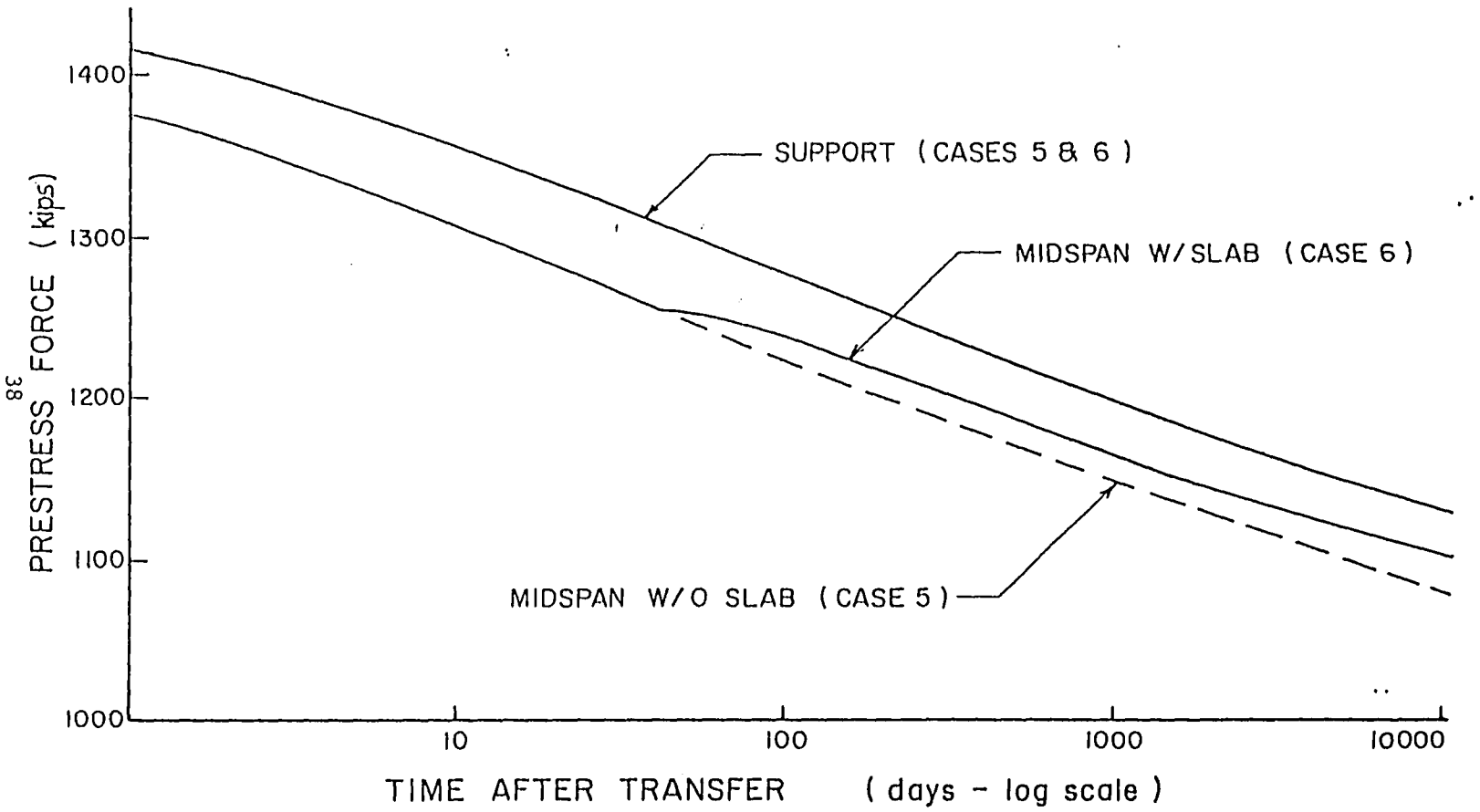

Figure 6: Variation of Prestress Force With Time- Parabolic Tendons

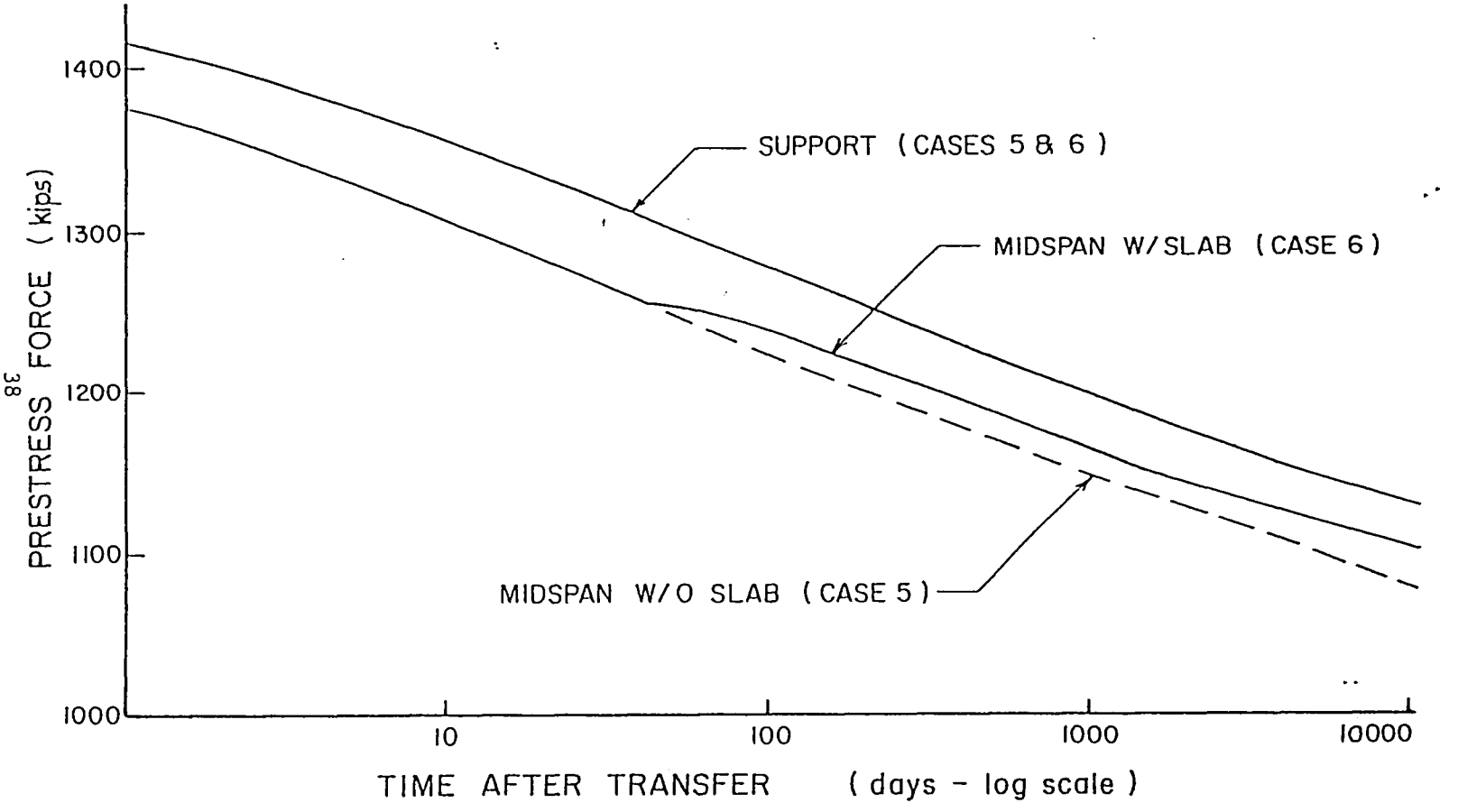

Figure 6: Variation of Prestress Force With Time- Parabolic Tendons

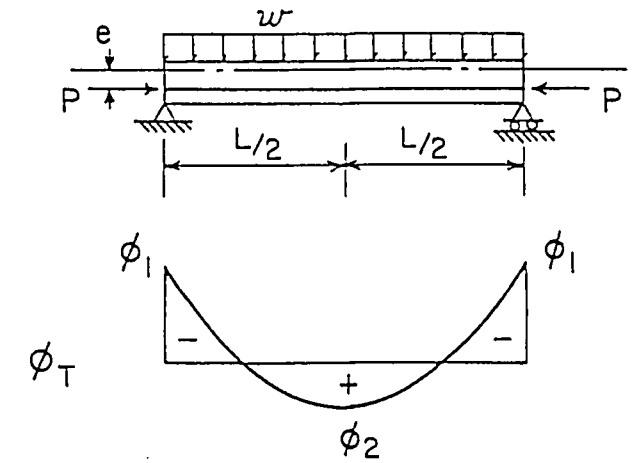

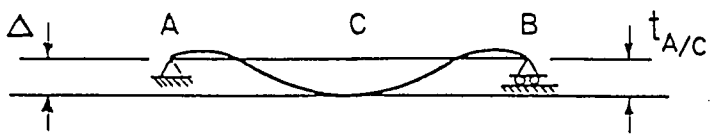

$$\Delta = t_{A/C} = \frac{L^2}{48}(\phi_1 + 5\phi_2)$$

Figure 7: Deflection by Moment-Area

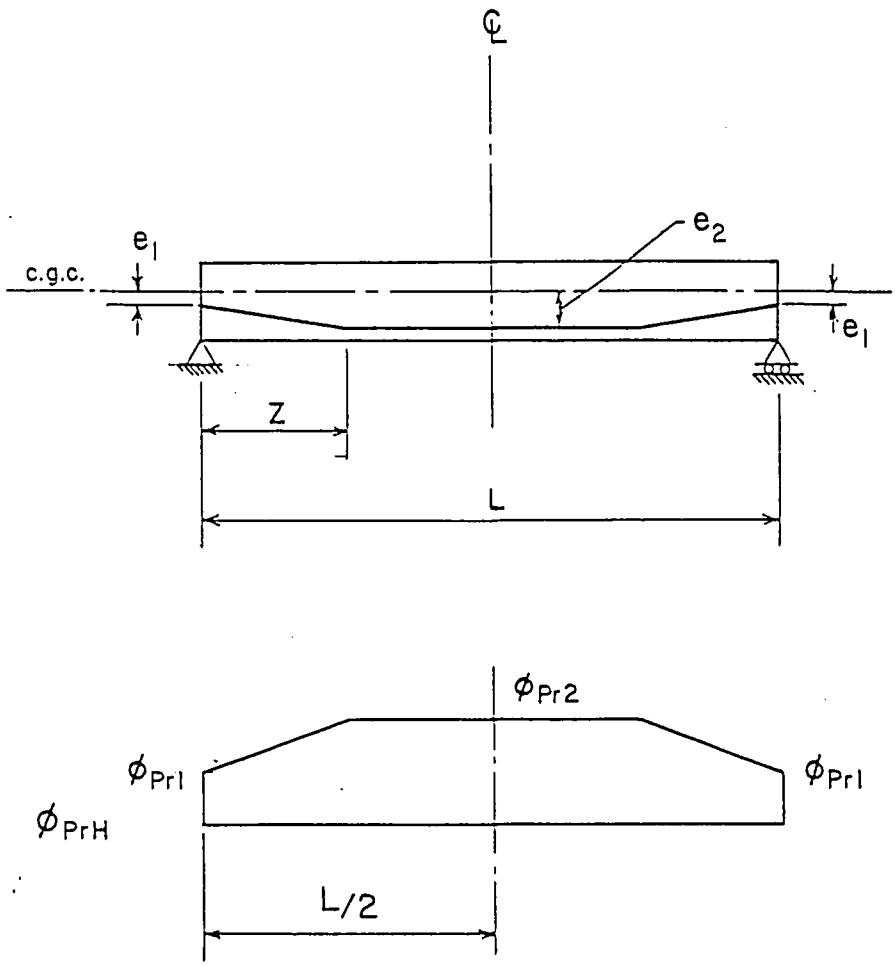

Figure 8: Prestress Curvature Diagram for a Harped Tendon Profile

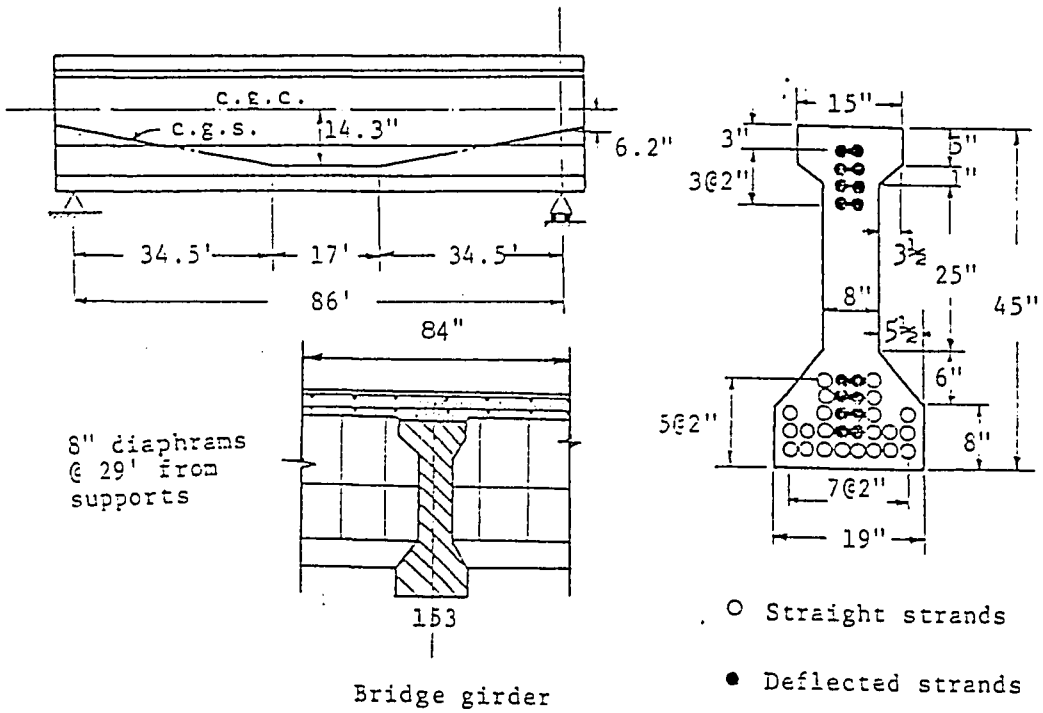

Concrete: girder- sand lightweight f'_c = 6100 psi
Slab - normal weight f'_c = 3500 psi
Girder Area = 515 in^2
Girder I = 108500 in^4

Steel: 270 K stress relieved strands
f_{si} = 190 ksi Area = 4.56 in^2
Transfer occurs at 3 days.

Diaphram moment = 680 kip-in added with the slab.

Slab cast at 65 days.

Figure 9: Example 1- Bridge Girder

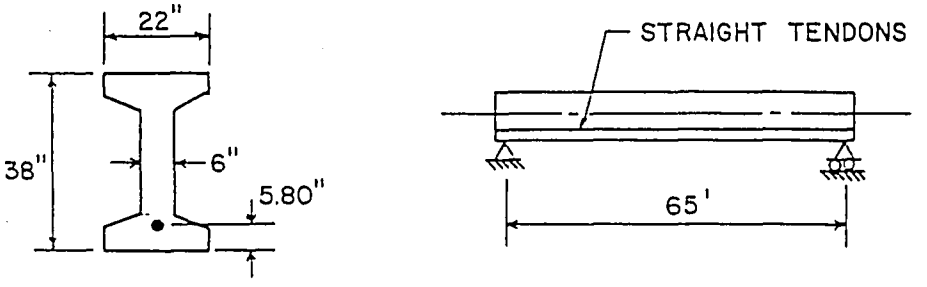

Concrete: normal weight f'_c = 6000 psi
Area = 452 in^2
I = 82170 in^4

Steel: 270 K stress relieved strands
20 - 1/2 inch diameter strands = 3.06 in^2

$f_{si} = 0.75\ f_{pu}$

Transfer occurs at 2 days after curing.

Loads: Selfweight = 0.470 k/ft.

Additional load = 1.0 k/ft

applied to the beam at 28 days

Figure 10: Example 2- Idealized Beam

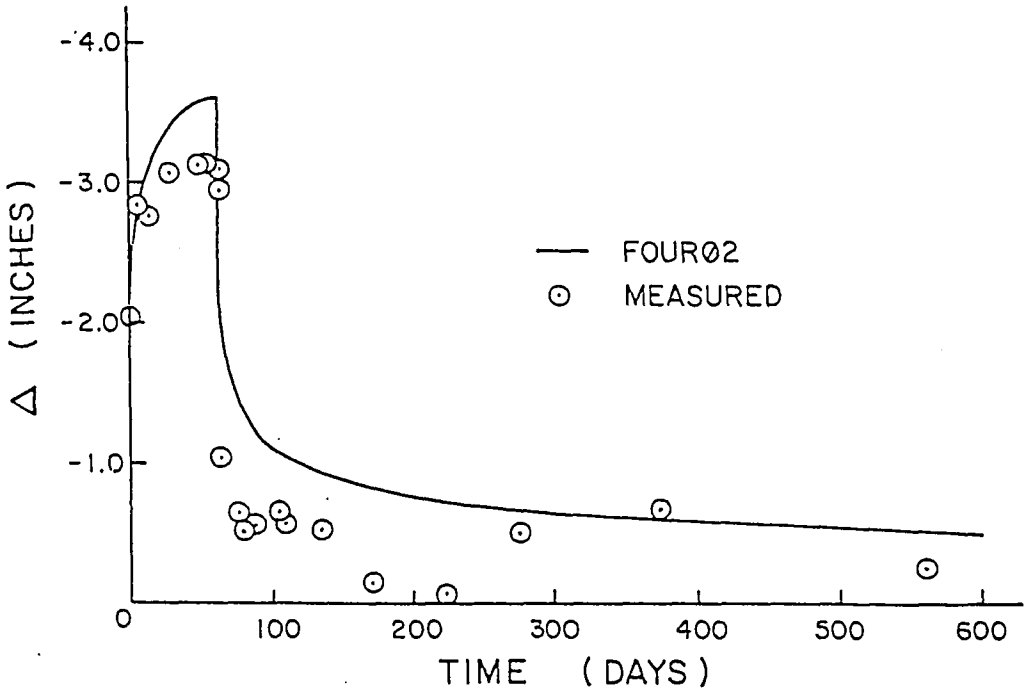

Figure 11: Results of Example 1- Bridge Girder

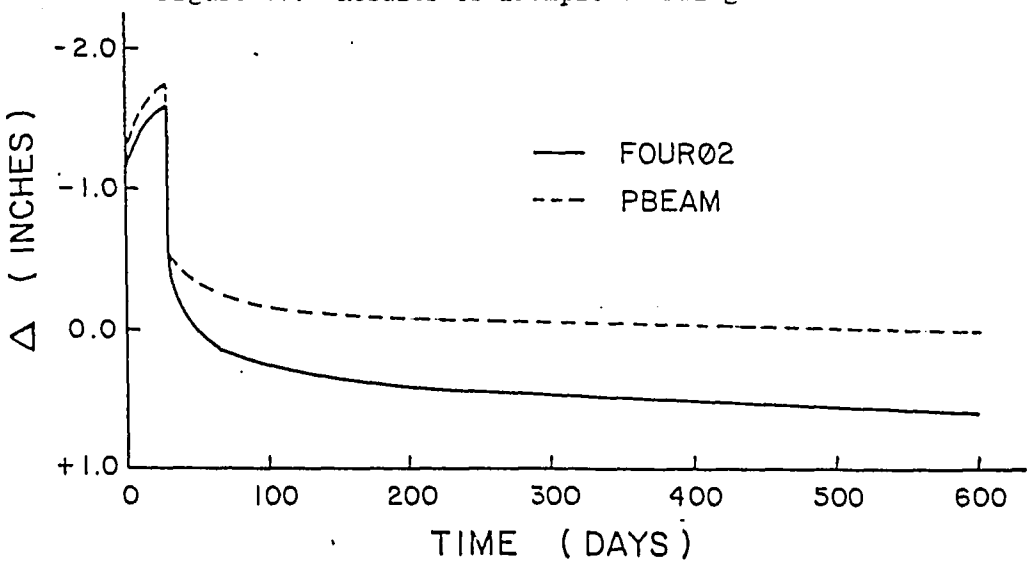

Figure 12: Results of Example 2- Idealized Beam

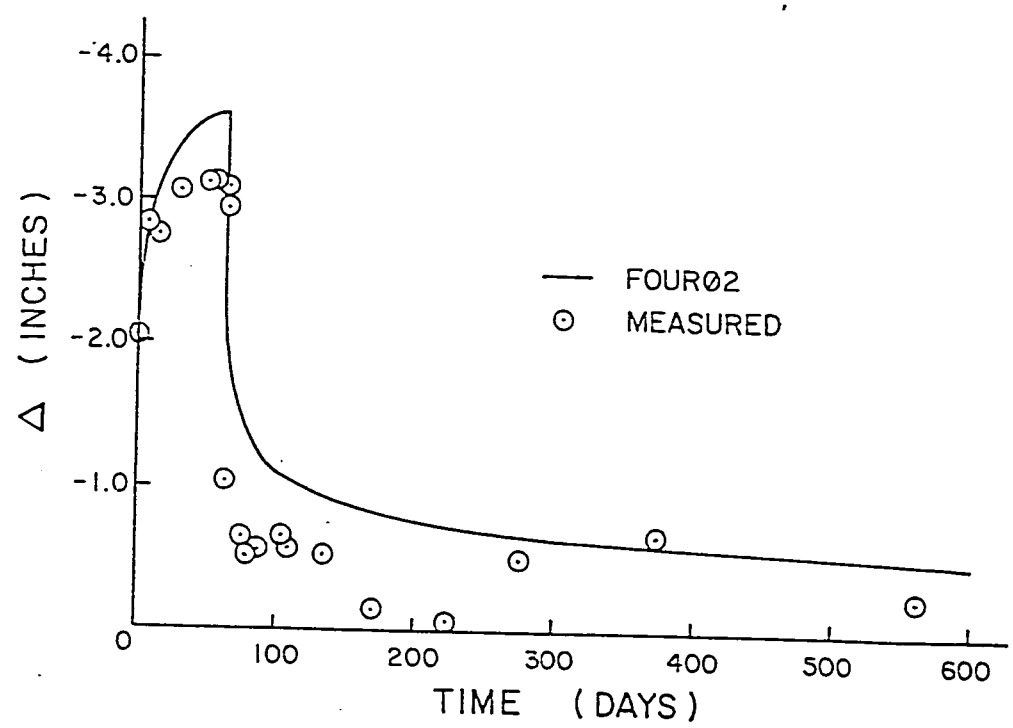

Figure 11: Results of Example 1- Bridge Girder

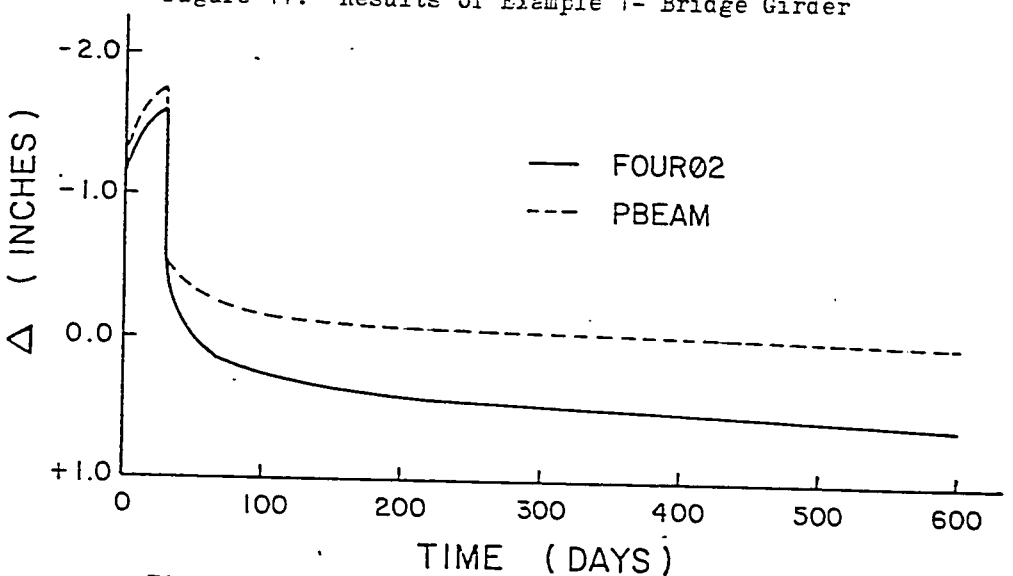

Figure 12: Results of Example 2- Idealized Beam

REFERENCES

1. Nilson, A. H., Design of Prestressed Concrete, John Wiley and Sons, 1978.

2. Huang, Ti, ``A New Procedure for Estimation of Prestress Losses,'' Fritz Engineering Laboratory Report No. 470.1, Lehigh University, 1982.

3. Huang, Ti and Hoffman, Burt, ``Prediction of Prestress Losses in Post-Tensioned Members,'' Fritz Engineering Laboratory Report No. 402.3, Lehigh University, December 1979.

4. Branson, Dan E., Deformation of Concrete Structures, McGraw-Hill, Inc., 1977.

5. Huang, Ti, ``Estimation of Prestress Losses in Concrete Bridge Members,'' Fritz Engineering Laboratory tory Report No. 402.4, Lehigh University, January 1980.

6. Huang, Ti, ``Prestress Losses in Pretensioned Concrete Structural Members,'' Fritz Engineering Laboratory Report No. 339.9, Lehigh University, August 1973.

7. Branson, D. E., Meyers, B. L., and Kripanarayanan, K. M., ``Time-Dependent Deformation of Non-Composite and Composite Prestressed Concrete Structures,'' Highway Research Board Report No. 70-1, University of Iowa, January 1970.

8. Lin, T. Y. and Burns, Ned H., Design of Prestressed Concrete Structures, John Wiley and Sons, 1981.

APPENDIX A. NOTATION

C_u = ultimate creep coefficient.

e_r = eccentricity of pretensioning prestress force, positive in the positive y-direction.

h = depth of the beam, inches.

I_c = net concrete moment of inertia.

L = span length.

P_e = ultimate prestress force after all losses.

P_i = initial prestress force at transfer.

P_{mid} = prestress force at midspan.

P_{sup} = prestress force at the support.

P_r = prestress force due to pretensioning stages.

R_t = correction factor for harped tendons.

S_{c1} = concrete strain at the top of the beam, contraction positive.

S_{c2} = concrete strain at the bottom of the beam, contraction positive.

S_{ci} = strain in concrete upon transfer of prestress.

S_{crm} = creep strain at midspan.

S_{crs} = creep strain at the support.

S_D = strain at the level of steel caused by the application of sustained loads.

$t_{A/C}$ = tangential deviation of point C with respect to point A. (See figure 7)

z = distance from support to the harping point of pretension stages.

Δ = midspan deflection.

Δ_D = deflection due to all sustained loads, including selfweight.

Δ_{pe} = deflection at the ultimate stage due to P_e.

Δ_{pi} = initial deflection due to P_i.

Δ_T = total midspan deflection for all stages.

Δ_{PrH} = deflection due to prestress of harped tendons.

Δ_{PsP} = deflection due to prestress of parabolic tendons.

Δ_{PrP} = deflection due to pretensioning of parabolic tendons.

Φ = curvature, in^{-1}.

Φ_1 = total curvature of support section.

Φ_2 = total curvature of midspan section.

Φ_{D2} = curvature at midspan caused by sustained loads, including selfweight.

Φ_{Pr} = curvature caused by pretensioning force.

Φ_{Ps} = curvature caused by post-tensioning stages.

APPENDIX B. PROCEDURE TO ESTIMATE PRESTRESS LOSSES

The basic procedure was developed initially for pretensioned members and later expanded to include post-tensioned members as well. The procedure makes use of experimentally established stress-strain - time characteristic equations of steel and concrete materials. These equations are linked by time and strain compatibility relationships, the equilibrium conditions, and a linear equation defining the distribution of concrete stresses across the member section. A direct solution of the stress and strain conditions at any time is then possible. Details of this procedure were presented in references 2, 3, 5 and 6. A very brief resume of the procedure is presented here. This procedure forms the basis of the computer program FOURO2 which deals with several types of prestressed concrete members.

The stress-strain-time relationship for prestressing steel is:

$$f_s = f_{pu} \{A_1 + A_2 S_s + A_3 S_s^2 - [B_1 + B_2 \log(t_s+1)]S_s - [B_3 + B_4 \log(t_s+1)]S_s^2\} \quad \text{(B-1)}$$

where: f_s = steel stress, in ksi.

f_{pu} = specified ultimate tensile strength of steel, in ksi.

S_s = steel strain, in 10^{-2}.

t_s = steel time, starting from tensioning, in days.

The coefficients A and B, which were obtained by a regression analysis of experimental data, are shown in Table 3. The terms with the A coefficients represent the instantaneous stress-strain relationship. The time-related relaxation loss of the steel stress is represented by the terms with B coefficients. Note that different steels may be used in the same member.

The stress-strain-time relationship for concrete is

$$\begin{aligned} S_c = & -C_1 f_c + [D_1 + D_2 \log(t_c+1)] \\ & + [E_1 + E_2 \log(t_c - t_{s1}+1)] - f_c E_3 \\ & - E_4(f_c - \Sigma f_{sdi}) \log(t_c - t_{s1}+1) \\ & - E_4 \Sigma[f_{sdi} \log(t_c - t_{si}+1)] \end{aligned} \qquad \text{(B-2)}$$

where

S_c = concrete strain, in 10^{-2}, contraction positive.

f_c = concrete stress, tension positive, in ksi.

t_c = concrete time, starting from the time when curing is terminated, in days.

t_{si} = age of concrete when the i-th stage stress increment is applied, in days.

f_{sdi} = increment of concrete stress at the i-th stage, in ksi.

In Equation (B-2), the first term on the right hand side, $-C_1 f_c$, represents the elastic strain, the second term, with D

coefficients, represents shrinkage, and the remaining terms with E coefficients represent the creep strain. The summation operations cover all stress increments which have already taken place at the time in question ($t_{si} \leqslant t_c$). The empirical coefficients C, D, and E for concretes commonly used for prestressed concrete bridge members in Pennsylvania are shown in Table 4.

The stress increments f_{sdi} are evaluated by an iterative procedure considering the conditions before and after the application of load or post-tensioning.

The compatibility conditions are

$$(t_s)_i = t_c - t_{si} \tag{B-3}$$

and

$$S_{si} + S_{ci} = k_{4i} \tag{B-4}$$

Here

$(t_s)_i$ = length of relaxation time for steel elements of the i-th stage.

k_{4i} = strain compatibility constant, in 10^{-2}.

S_{si} and S_{ci} are concurrent steel and concrete strains.

For pretensioned tendons, S_{ci} is zero immediately before transfer. Consequently, k_{4i} is a controlled input equal to the

initial jacking strain. For post-tensioned tendons, evaluation of k_{4i} is somewhat more complex. At the post-tensioning time t_{si}, S_{si} is the tensioning strain in steel of the i-th stage, which is directly under control and known. The corresponding S_{ci}, however, is not a controlled input. It includes the effects of all prestressing and loading up to and including the i-th stage, and is calculated by an iterative process. The constant k_{4i} is determined by adding S_{si} and S_{ci} at time t_{si}, and is maintained constant for all subsequent time.

The equilibrium equations are

$$\int f_c \, dA + \Sigma(f_{si} \, a_{si}) = -P \qquad \text{(B-5)}$$

$$\int f_c \, y \, dA + \Sigma(f_{si} \, a_{si} \, y_i) = M \qquad \text{(B-6)}$$

where:

A = area of net concrete section, in sq. in.

a_{si} = area of prestressing steel of i-th stage, in sq. in.

y_i = distance to elementary area from the centroidal horizontal axis, in inches.

P = applied axial load on the section, kips.

M = applied bending moment on the section, kip-in.

The positive directions of y, P, and M are shown in Figure 1. The integrations are over the net concrete area and the summations are over all steel elements which have already been tensioned and anchored to the member.

A linear distribution of concrete stresses (corresponding to a linear strain distribution) is considered

$$f_c = g_1 + g_2 y \tag{B-7}$$

where g_1, g_2 = parameters to define concrete stress distribution.

Combination of equations (B-1), (B-2), (B-3), and (B-4) shows that the steel stress in any given element, f_{si}, can be expressed as a quadratic function of the concurrent concrete stress, f_{ci}.

$$f_{si} = R_{1i} + R_{2i} f_{ci} + R_{3i} f_{ci}^2 \tag{B-8}$$

where the R coefficients are functions of the material properties, the compatibility constants and the time parameter t_c [3]. Substituting Equation (B-7) into the equilibrium conditions and integrating,

$$Ag_1 + \Sigma(f_{si}\, a_{si}) = -P \tag{B-9}$$

$$Ig_2 + \Sigma(f_{si}\, a_{si}\, y_i = M \tag{B-10}$$

Substitution of Equations (B-7) and (B-8) into (B-9) and (B-10) results in two quadratic equations of g_1 and g_2 which can be solved simultaneously. The stresses and strains are then determined by back substitution.

APPENDIX C. DERIVATION OF EQUATIONS

C.1 Parabolic Fit of Curvature Diagram

The general equation of the parabola is

$$\Phi = a_1 + a_2 z + a_3 z^2 \qquad \text{(C-1)}$$

where

Φ = the curvature.

z = distance along the span (see Fig. 1).

a_1, a_2, a_3 are the coefficients to be determined.

To determine the unknown coefficients, three boundary conditions are used. Namely,

1. at $z=0$, $\Phi=\Phi_1$ = curvature at one support.
2. at $z=L/2$, $\Phi=\Phi_2$ = curvature at midspan.
3. at $z=L$, $\Phi=\Phi_1$ = curvature at other support.

Applying these boundary conditions to equation (C-1), we obtain:

$$a_1 = \Phi_1 \qquad \text{(C-2)}$$

$$a_2 = \frac{4\,(\Phi_2 - \Phi_1)}{L} \qquad \text{(C-3)}$$

$$a_3 = \frac{-4\,(\Phi_2 - \Phi_1)}{L^2} \qquad \text{(C-4)}$$

Thus the equation of the parabolic approximation is found.

C.2 Midspan Deflection By Moment-Area

The tangential deviation $t_{A/C}$, as shown in Figure 7, can be computed by taking the first moment of the curvature diagram from midspan to the support about the support.

$$t_{A/C} = \int_{L/2}^{0} \Phi z \, dz = \int_{L/2}^{0} (a_1 + a_2 z + a_3 z^2) z \, dz \qquad (C\text{-}5)$$

Performing this integration and then substituting equations (C-2), (C-3), and (C-4) into (C-5) gives equation (4-1).

$$\Delta = \frac{L^2}{48} (\Phi_1 + 5\Phi_2) \qquad (4\text{-}1)$$

C.3 Correction Factor R_t

By applying the moment-area method to the harped curvature diagram (Figure 8) we can find the corresponding prestress deflection to be

$$\Delta_{PrH} = \frac{1}{48} [8\Phi_{Pr1} z^2 + \Phi_{Pr2}(6L^2 - 8z^2)] \qquad (C\text{-}6)$$

Substituting (C-6) and (4-8) into (4-3) and reducing gives equation (4-4).

The pretensioning curvature, Φ_{Pr}, is determined by applying a force, equal to the pretensioning force, to the net concrete section. The resulting stresses are found from the equation

$$f_c = \frac{-P_r}{A_c} - \frac{P_r e_r y}{I_c} \qquad (C\text{-}7)$$

where

A_c = net area of concrete.

Figure 1 shows the positive direction of P_r. The eccentricity e_r is taken as positive in the positive y-direction. Tension in concrete is positive.

The concrete strain is found from equation (B-2) rewritten in the form

$$S_c = Q_1 - Q_2 f_c \qquad (C\text{-}8)$$

where

$$Q_1 = [D_1 + D_2 \log(t_c+1)] + [E_1 + E_2 \log(t_c - t_{s1}+1)] - E_4 \sum\{f_{sdi}[\log(t_c - t_{si}+1) - \log(t_c - t_{s1}+1)]\}$$

$$Q_2 = C_1 + E_3 + E_4 \log(t_c - t_{s1}+1)$$

The top and bottom fiber strains are computed using (C-7) and (C-8), and substituted into equation (2-2) to obtain (4-12).

$$\Phi_{Pr} = \frac{-Q_2 P_r e_r y}{100\, I_c} \qquad (4\text{-}12)$$

The factor of 100 results because strain is defined in 10^{-2} in the concrete equation (B-2).

VITA

The author was born to Charles and Elizabeth Stumpp in New York City on January 19, 1959. He grew up in Norwalk, Connecticut and attended Norwalk High School. Upon graduation from high school in June of 1977, he began study at Lehigh University. In May of 1981 he received a Bachelor of Science Degree in Civil Engineering. While at Lehigh he became a member of Tau Beta Pi and Chi Epsilon.

In August of 1981, the author returned to Lehigh to pursue graduate studies in Civil Engineering. There he taught computer programming and numerical methods for three semesters as a teaching assistant. He will be graduated in October of 1983 with a Master of Science Degree in Civil Engineering.